Polymer Chemistry

ROYAL SOCIETY OF CHEMISTRY

PAPER

View Article Online
View Journal | View Issue



Cite this: *Polym. Chem.*, 2025, **16**, 3258

# Creation of polymersomes with changes in the membrane structure *via* disulfide crosslinking under reductive conditions for controlled gradual cargo release†

Tomoya Kojima, Kouichi Asakura and Taisuke Banno *

The controlled release of cargo from carriers is a critical challenge in drug delivery. Polymersomes are capsule-like structures self-assembled from amphiphilic polymers that can function as carriers. Although the sudden release of cargo has been achieved by inducing the overall structural collapse of polymersomes, the gradual release of cargo, which is key for decreasing the number of drug-administration cycles, remains a challenge. Disulfide crosslinking is one of the candidates for controlling the releasing ability of polymersomes. However, such previous research only focused on strategies for oxidation of thiol to induce disulfide crosslinking under oxidative conditions, which missed the potential for the disulfide crosslinking under reductive conditions. Herein, we realize a new strategy that disulfide crosslinking can be induced under reductive conditions. Amphiphilic polymers with multiple disulfide bonds were newly synthesized, and they self-assembled into polymersomes that facilitate the gradual release of cargo in a reductive environment. The addition of glutathione facilitated the successive crosslinking of the disulfide bonds in the membranes, resulting in a rigidified membrane structure. The changes in the membrane rigidity influenced the permeability of the cargo in the polymersome, resulting in its controlled release. We expect that our study will expand molecular design strategies to control the membrane properties of polymersomes.

Received 17th March 2025,
Accepted 17th June 2025

DOI: 10.1039/d5py00273g

rsc.li/polymers



## Introduction

Polymersomes are vesicles composed of multiple amphiphilic block copolymers.[1–4] As they have a capsule-like structure and their inner chamber can be loaded with cargo molecules, they can be applied as carriers.[5–7] Considering the application of polymersomes as carriers of cargo, it is important to regulate the permeability and disruption of polymersome membranes, because the cargo molecules are not only required to be stably retained in the polymersomes without leakage, but also released controllably at the targeted time and space.[8,9] Polymersomes comprising macromolecules have various advantages, including a high stability and mechanical rigidity,[10] over liposomes comprising low-molecular-weight amphiphiles. Moreover, a key characteristic of polymersomes is their chemical versatility.[11–13] The molecular structures of amphiphilic polymers can be designed flexibly in terms of their molecular weight, degree of polymerization, and side chains, thereby modulating the properties of polymersome membranes. Thus, the permeability and disruption of their membranes can be controlled by precisely designing the molecular structures of amphiphilic polymers.

To regulate the permeability and disruption of polymersome membranes using external stimuli, various stimuli-responsive polymersomes have been developed.[14–16] Moreover, different types of external stimuli, such as pH,[17–19] ions,[20] temperature,[21] light,[22–24] magnetic field,[25] and ultrasound,[26] have been used depending on the targeted application. Among the various candidates, redox-responsive polymersomes have drawn considerable attention because of the abundance of redox compounds in biological environments, considering the application of polymersomes as carriers in biological systems.[27–29]

A key challenge in the development of smart carriers is to control the release of cargo at desired speeds and on demand. Most of the conventional studies have mainly focused on designing amphiphilic polymers that self-assemble into polymersomes that completely collapse in response to external stimuli, not realizing the gradual release of cargo. To overcome this problem, dual or triple stimuli-responsive polymersomes that exhibit changes in the membrane permeability in

*Department of Applied Chemistry, Keio University, 3-14-1 Hiyoshi, Kohoku-ku, Yokohama, Kanagawa, 223-8522, Japan. E-mail: tbanno@keio.jp*

† Electronic supplementary information (ESI) available. See DOI: https://doi.org/10.1039/d5py00273g

response to a specific stimulus, have been prepared.[30–33] Other studies have demonstrated that gels can be used in the inner part of the polymersomes to delay the diffusion of cargo molecules.[34,35]

Crosslinking is an effective method for improving the structural stability of polymersome membranes; however, it leads to decreased membrane permeability. Previously, the crosslinking of polymers *via* the polycondensation of siloxane,[36] free-radical polymerization of butadiene,[37] and ionic complex formation,[38] has been reported. Further, a recent study presented the concept of "traceless crosslinking", demonstrating that both the stability of the membrane structure against collapse and the cargo release can be balanced using this strategy.[39–42] In the traceless crosslinking strategy, an external stimulus was used to first induce the cleavage of the polymer chains; however, successive amidation reactions induced crosslinking, which led to membrane stability as well as hydrophobic-to-hydrophilic transition within membrane, leading to the permeation of the loaded cargo. Thus, crosslinking reactions are not only beneficial for membrane stability but also for cargo release.

In this study, we aimed to achieve the gradual release of cargo from polymersomes under redox conditions by promoting disulfide crosslinking within the membrane. While previous studies have demonstrated redox-responsive molecular self-assemblies consisting of amphiphilic polymers with disulfide moieties in the main and side chains,[43–48] they primarily relied on thiol oxidation under oxidative conditions, often leading to membrane disruption upon exposure to reductants like glutathione (GSH), a thiol-containing tripeptide that is abundant in cells. In contrast, we focused on disulfide exchange reactions under reductive conditions by designing amphiphilic polymers with multiple disulfide bonds in the hydrophobic side chains (Fig. 1a). The close proximity of disulfides in the membrane enabled GSH to trigger not only the cleavage of the disulfide bonds but also successive disulfide exchange reactions, resulting in the crosslinking of the polymersome membrane (Fig. 1b). This increased the membrane rigidity and reduced membrane permeability, thereby allowing the controlled gradual cargo release.

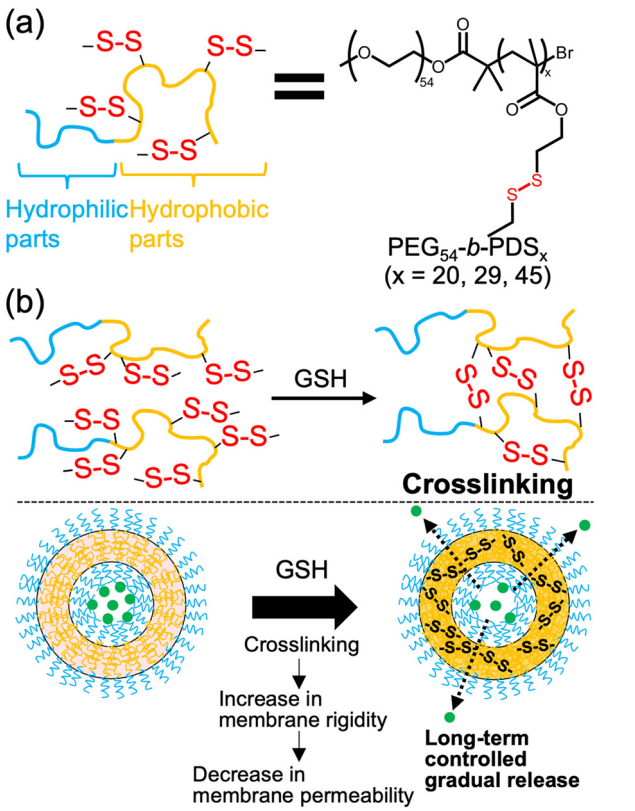


**Fig. 1** Redox-responsive polymersomes. (a) Amphiphilic polymers with multiple disulfide bonds. (b) Conceptual illustration of this study.

## Results and discussion

### Synthesis of amphiphilic polymers with multiple disulfide bonds

Amphiphilic polymers containing multiple disulfide bonds at the side chains of the hydrophobic parts (Fig. 1a), that is block copolymers with polyethylene glycol (PEG) and poly-disulfide units (PDS) $PEG_{54}$-*b*-$PDS_x$ with $x$ = 20, 29, and 45, were synthesized as follows: macroinitiators containing hydrophilic polyethylene oxide chains (Fig. S1 and Table S1†) and monomers with disulfide bonds in their hydrophobic parts (Fig. S2–S5†) were polymerized *via* atom transfer radical polymerization. The monomer ratio was adjusted based on the weight fraction of the hydrophilic blocks (20–40%) that is favorable for forming vesicles based on previous reports.[49] Amphiphilic polymers with three different degrees of polymerization were synthesized to investigate the effect of the number of disulfide bonds in the polymer on the permeability of the polymersome membrane. The degree of polymerization of the obtained polymers, $PEG_{54}$-*b*-$PDS_x$, was analyzed using $^1$H NMR spectroscopy (Fig. S6–S8†). Comprehensive characterization was conducted using gel permeation chromatography (GPC) (Table S2†).

### Preparation and characterization of polymersomes

Polymersomes were prepared from the synthesized amphiphilic polymers using the solvent injection method.[50,51] In brief, aqueous Tris-HCl buffer (pH 7.4) was gradually injected into the polymer solution in tetrahydrofuran (THF)/1,4-dioxane (4/1 v/v) using a syringe pump (1.0 mL min$^{-1}$) with stirring. The obtained suspensions were then dialyzed overnight to remove the organic solvents. After dialysis, the samples were characterized using transmission electron microscopy (TEM) and dynamic light scattering (DLS). The TEM images show the formation of nanometer-sized capsule-like structures (Fig. 2 and Fig. S9†). DLS measurements also revealed that nanoscale molecular assemblies were mainly formed (Fig. S10†), indicating that all three amphiphilic polymers formed nanometer-sized polymersomes. Since polymersomes were prepared using solvent injection techniques, the polymersomes were at nano-

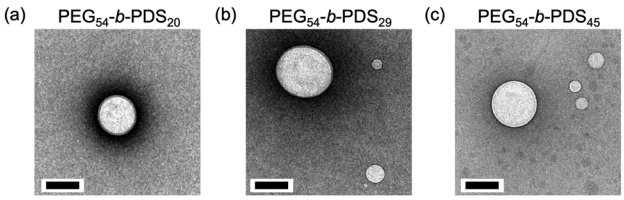


Fig. 2 TEM images of polymersomes comprising (a) $PEG_{54}$-*b*-$PDS_{20}$, (b) $PEG_{54}$-*b*-$PDS_{29}$, and (c) $PEG_{54}$-*b*-$PDS_{45}$. Scale bars: 200 nm.

meter scale, and the size distribution was polydisperse and not well-controlled.

### Reaction analysis

The molecular conversion of the amphiphilic polymers was investigated by adding GSH. The polymersome suspensions in Tris-HCl buffer (pH 7.4) were mixed with GSH solutions and incubated at 37 °C for 6 h. The samples were then lyophilized to remove water, and THF was added. Because the Tris-HCl salt is insoluble in THF, only the supernatant was used for

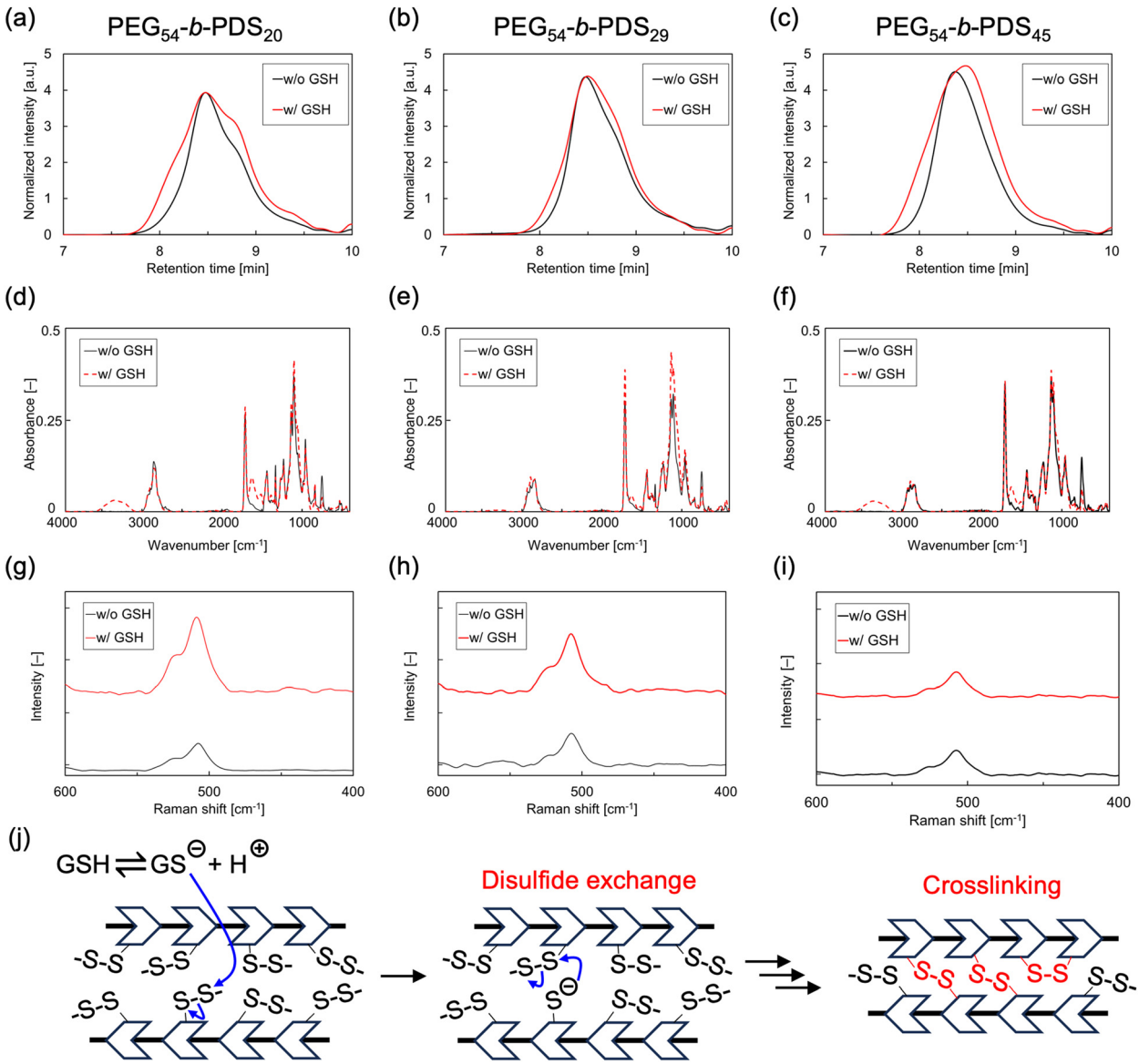


Fig. 3 Analysis of the changes in $PEG_{54}$-*b*-$PDS_x$ ($x$ = 20, 29, and 45) with the addition of GSH. (a–c) GPC curves of (a) $PEG_{54}$-*b*-$PDS_{20}$, (b) $PEG_{54}$-*b*-$PDS_{29}$, and (c) $PEG_{54}$-*b*-$PDS_{45}$ with/without GSH. (d–f) Infrared spectra of (d) $PEG_{54}$-*b*-$PDS_{20}$, (e) $PEG_{54}$-*b*-$PDS_{29}$, and (f) $PEG_{54}$-*b*-$PDS_{45}$ with/without GSH. (g–i) Raman spectra of (g) $PEG_{54}$-*b*-$PDS_{20}$, (h) $PEG_{54}$-*b*-$PDS_{29}$, and (i) $PEG_{54}$-*b*-$PDS_{45}$ with/without GSH. (j) Estimated molecular conversions of the polymers after the addition of GSH. Thiolate anions of GSH attack the disulfide bonds in the polymer chains to generate new thiolate anions. Subsequently, the generated thiolate anions, which are reactive, attack other disulfide bonds. Chain reactions involving such disulfide exchange reactions result in the overall crosslinking of the polymers.

 

GPC analysis to eliminate the Tris-HCl salt. The GPC curves (Fig. 3a–c) reveal that the molecular-weight distributions of the polymers changed after the addition of GSH, indicating the occurrence of molecular conversions that changed their molecular weights. The results indicated that polymers of both high and low molecular weights were generated after the addition of GSH.

To further investigate the molecular conversions in $PEG_{54}$-*b*-$PDS_x$, we analyzed the infrared (IR) and Raman spectra of the solids obtained by evaporating THF from the supernatant used for GPC. The IR spectra do not exhibit the S–H stretching vibrational peak of free thiol groups at 2500–2600 $cm^{-1}$ even after the addition of GSH, indicating the absence of free thiol (–SH) residues in the polymers (Fig. 3d–f). In the Raman spectra, the peak of the S–S stretching vibration derived from disulfide bonds was detected at approximately 500 $cm^{-1}$ even after the addition of GSH, indicating that the disulfide bonds were preserved in the polymers (Fig. 3g–i).

These results suggest that not only a simple reduction of the disulfide linkages in the polymers into free thiols, but also further oxidation of the generated thiols (that is, disulfide exchange reactions) occurred in the chemical systems. Based on these results, the possible molecular conversions are illustrated in Fig. 3j. At pH 7.4, a portion of GSH is ionized to generate thiolate anions, because the p$K_a$ of GSH is 8.93.[52] The anions attack the disulfide bonds in the polymers to generate thiolate anions at their side chains. Because the amphiphilic polymers formed polymersomes, their hydrophobic parts were highly packed within the polymersome structure. Thus, the generated thiolate anions attack neighboring disulfide bonds. Such disulfide exchange reactions can occur as chain reactions anywhere in the membrane, resulting in the crosslinking of the polymer molecules. Because some of the disulfide bonds in the polymers were reduced and intramolecular crosslinking occurred, a decrease in the molecular weight was also observed, as demonstrated through GPC measurements.

### Effects of GSH on polymersomes

To investigate the influence of such molecular crosslinking on the structural properties of the polymersomes, we performed TEM and DLS analyses of the samples obtained after the incubation of the polymersome suspensions in Tris-HCl buffer (pH 7.4) with GSH solutions at 37 °C for 6 h. TEM observations revealed that the nanoscale capsule-like structures of the polymersomes were maintained after their reaction with GSH (Fig. 4 and Fig. S11†). DLS measurements also revealed the presence of nanoscale molecular self-assemblies (Fig. S12†). These results clearly revealed that the polymersomes retained their shape even after GSH addition.

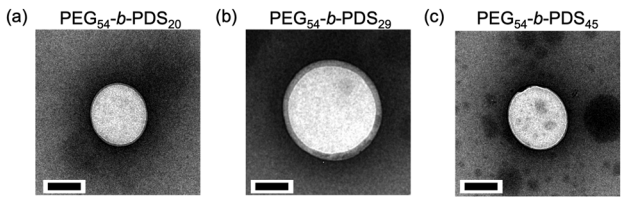


**Fig. 4** TEM images of polymersomes comprising (a) $PEG_{54}$-*b*-$PDS_{20}$, (b) $PEG_{54}$-*b*-$PDS_{29}$, and (c) $PEG_{54}$-*b*-$PDS_{45}$ after incubation with GSH (5 mM) in Tris-HCl buffer for 6 h. Scale bars: 200 nm.

After having confirmed that the polymersomes did not collapse in the presence of GSH, changes in their membrane structure were investigated. Nile Red is an environmentally responsive fluorescent probe that exhibits a change in its fluorescence intensity and fluorescence peak shift depending on the polarity of the environment.[53,54] The results of Nile Red-added polymersome suspensions revealed an increase in the fluorescence intensity and peak shift of Nile Red to a lower wavelength after GSH addition, indicating that GSH induced a decrease in the polarity of the membrane environment (Fig. S13†).

Further, to evaluate the changes in the membrane structure more quantitatively, another method based on the evaluation of the generalized polarization (GP) of a fluorophore was employed. Laurdan is an environmentally responsive fluorescent probe, and its GP value is calculated as $(I_{440\ nm} - I_{490\ nm})/(I_{440\ nm} + I_{490\ nm})$, where $I_{440\ nm}$ and $I_{490\ nm}$ are the fluorescence intensities at 440 and 490 nm, respectively.[55] GP corresponds to membrane fluidity, and GP increases as the fluidity of the membrane decreases. Fluorescence measurements on Laurdan-incorporated polymersomes revealed that the GP of Laurdan increased in all the amphiphilic polymers after the addition of GSH, indicating that the membrane fluidity decreased in the presence of GSH (Fig. 5a–c). The time course of the GP of Laurdan incorporated in the $PEG_{54}$-*b*-$PDS_{29}$ polymersome revealed that the membrane fluidity decreased gradually over time (Fig. 5d). Based on the proposed mechanism of molecular conversion, the membrane fluidity decreases owing to polymer crosslinking caused by successive disulfide exchange reactions in the membranes.

### Cargo release assay

Finally, the influence of the changes in the membrane fluidity on the release of the cargo loaded into the polymersomes was investigated using fluorescent dye calcein as a model cargo.[56,57] It was confirmed that the calibration curve was constructed where fluorescence intensity of calcein was proportional to the concentration, showing that the release of calcein was estimated by measuring the fluorescence intensity (Fig. S14†). Calcein was incorporated into polymersomes during their synthesis using the solvent injection method, and the excess calcein, which was not incorporated in the polymersomes, was removed by dialyzing the sample overnight. Based on the calibration curve, both encapsulation efficiency (EE) and loading content (LC) were determined for $PEG_{54}$-*b*-$PDS_x$ polymersomes. EE, defined as the ratio of loaded calcein to the initial amount of calcein, was approximately 30 wt%, while LC, defined as the ratio of the loaded calcein to the total polymer weight, was approximately 3 wt%. These values were consistent regardless of the degree of polymerization (Table S3†). Next, the cargo-release properties of the polymer-

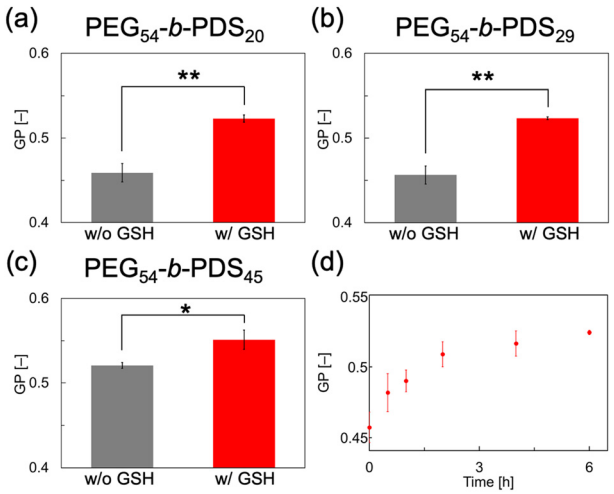


**Fig. 5** Changes in $PEG_{54}$-*b*-$PDS_x$ membrane structures with GSH addition. (a–c) GP values calculated using the fluorescent intensity of Laurdan incorporated in polymersomes comprising (a) $PEG_{54}$-*b*-$PDS_{20}$, (b) $PEG_{54}$-*b*-$PDS_{29}$, and (c) $PEG_{54}$-*b*-$PDS_{45}$ with/without GSH. (d) Time course of the changes in the GP of Laurdan in the $PEG_{54}$-*b*-$PDS_{29}$ polymersomes after the addition of GSH. *p* values were calculated based on student's *t*-test. $*p < 0.05$, $**p < 0.01$.

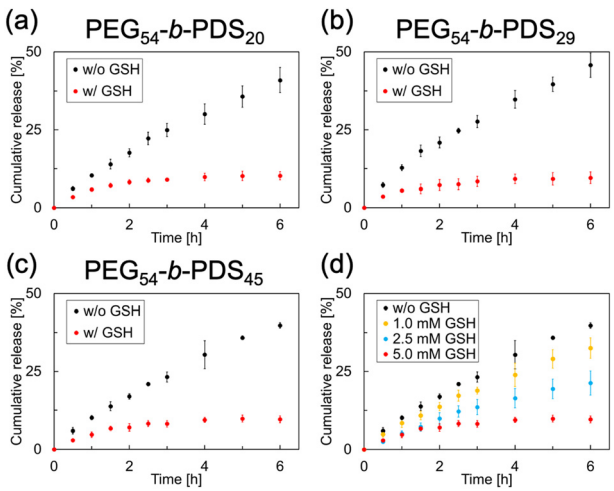


**Fig. 6** Release of calcein from polymersomes with/without GSH. (a–c) Cumulative release of calcein from polymersomes comprising (a) $PEG_{54}$-*b*-$PDS_{20}$, (b) $PEG_{54}$-*b*-$PDS_{29}$, and (c) $PEG_{54}$-*b*-$PDS_{45}$ with/without GSH (5 mM). (d) GSH-concentration-dependent cumulative release of calcein from polymersomes comprising $PEG_{54}$-*b*-$PDS_{45}$.

somes were investigated by measuring the fluorescence intensity of the released calcein (Fig. 6a–c). Compared with that in the absence of GSH, the speed of calcein release was delayed in the presence of GSH. In addition, the influence of GSH concentration was investigated using the $PEG_{54}$-*b*-$PDS_{45}$ polymersomes (Fig. 6d). The cargo-release rate was found to decrease more rapidly as the GSH concentration increased, indicating that the release rate could be controlled by varying the GSH concentration. The release rate did not depend on the degree of polymerization of the polymers, suggesting that a more significant change in the degree of polymerization is required to influence the changes in membrane properties and leakage of loaded cargo molecules by controlling crosslinking. In summary, the addition of GSH induced the crosslinking of the polymersome membrane by inducing successive disulfide exchange reactions between the self-assembled polymers, thereby decreasing the membrane fluidity and thus realizing the gradual release of the loaded cargo.

Previous research has predominantly emphasized strategies for oxidizing thiols to promote disulfide crosslinking under oxidative conditions, which neglected the possibility of disulfide crosslinking occurring under reductive conditions. In contrast, we discovered an unconventional approach, demonstrating that disulfide crosslinking can also be initiated under reductive conditions when multiple disulfides are closely positioned at the membranes of polymersomes. These findings offer valuable insights, broadening molecular design strategies to fine-tune the membrane properties of polymersomes.

## Conclusions

In conclusion, new amphiphilic polymers with multiple disulfide bonds in their side chains were prepared, and nanoscale polymersomes were formed from the synthesized polymers. The addition of GSH to the polymersomes induced successive disulfide exchange reactions in the crowded environment of the polymersome membrane structure, resulting in membrane crosslinking. The polymersomes retained their structure after the addition of GSH, and the crosslinking of the membrane decreased its fluidity, thereby inducing the gradual release of the loaded cargo. The release rate of the cargo could be controlled by changing the concentration of GSH used as the stimulus.

The controlled release of the loaded cargo is an important function of carriers. When carriers are ruptured using external stimuli, the loaded cargo molecules, such as drugs, are released at once. Compared to short-term release, the gradual release of the cargo is advantageous for continuously delivering a safe drug dose over a long time with only a single administration.[58] A decrease in the number of drug-administration cycles minimizes the pain and discomfort experienced by patients. It is known that the concentration of reducing agents, such as GSH, is higher in the cytosol of biological cells (1–10 mM) than in the blood (10–40 μM).[45] Thus, the redox-responsive polymersomes developed in this study have the potential to be used as carriers for delivering drugs to biological cells, realizing the gradual release of the loaded drug under reductive cytosolic environments.

## Author contributions

T. K. and T. B. conceived the experiments and led the project. T. K. performed the experiments. T. K., K. A., and T. B discussed the results. T. K. and T. B. wrote the manuscript.

## Conflicts of interest

There are no conflicts to declare.

## Data availability

All relevant data are available from the corresponding author upon reasonable request.

## Acknowledgements

This work was supported by JSPS KAKENHI Grant Numbers JP20H02712 and JP22KJ2723. T. K. was granted by the Keio University Doctorate Student Grant-in-Aid Program from Ushioda Memorial Fund.

## References

1 N. P. Kamat, J. S. Katz and D. A. Hammer, *J. Phys. Chem. Lett.*, 2011, **2**, 1612–1623.
2 S. Matoori and J.-C. Leroux, *Mater. Horiz.*, 2020, **7**, 1297–1309.
3 I. Ortiz-Rivera, M. Mathesh and D. A. Wilson, *Acc. Chem. Res.*, 2018, **51**, 1891–1900.
4 W. Li, S. Zhang, M. Sun, S. Kleuskens and D. A. Wilson, *Acc. Mater. Res.*, 2024, **5**, 453–466.
5 C. G. Palivan, R. Goers, A. Najer, X. Zhang, A. Car and W. Meier, *Chem. Soc. Rev.*, 2016, **45**, 377–411.
6 K. Kuperkar, D. Patel, L. I. Atanase and P. Bahadur, *Polymers*, 2022, **14**, 4702.
7 J. S. Lee and J. Feijen, *J. Control. Release*, 2012, **161**, 473–483.
8 S. Cao, T. Ivanov, M. de Souza Melchiors, K. Landfester and L. Caire da Silva, *ChemBioChem*, 2023, **24**, e202200718.
9 A. Kayani, A. Raza, J. Si, D. Dutta, Q. Zhou and Z. Ge, *Biomacromolecules*, 2023, **24**, 4622–4645.
10 Y. Luo, A. B. Cook, L. K. E. A. Abdelmohsen and J. C. M. van Hest, *Annu. Rev. Mater. Res.*, 2024, **54**, 75–96.
11 E. Rideau, R. Dimova, P. Schwille, F. R. Wurm and K. Landfester, *Chem. Soc. Rev.*, 2018, **47**, 8572–8610.
12 J. Lefley, C. Waldron and C. R. Becer, *Polym. Chem.*, 2020, **11**, 7124–7136.
13 M. Hasannia, A. Aliabadi, K. Abnous, S. M. Taghdisi, M. Ramezani and M. Alibolandi, *J. Control. Release*, 2022, **341**, 95–117.
14 H. Che and J. C. M. van Hest, *J. Mater. Chem. B*, 2016, **4**, 4632–4647.
15 T. Thambi, J. H. Park and D. S. Lee, *Biomater. Sci.*, 2016, **4**, 55–69.
16 O. Onaca, R. Enea, D. W. Hughes and W. Meier, *Macromol. Biosci.*, 2009, **9**, 129–139.
17 H. Che, S. Cao and J. C. M. van Hest, *J. Am. Chem. Soc.*, 2018, **140**, 5356–5359.
18 J. F. Mukerabigwi, W. Yin, Z. Zha, W. Ke, Y. Wang, W. Chen, A. Japir, Y. Wang and Z. Ge, *J. Control. Release*, 2019, **303**, 209–222.
19 M. Tollemeto, S. Ursulska, P. L. W. Welzen, L. H. E. Thamdrup, A. Malakpour-Permlid, Y. Li, G. Soufi, T. P. Padial, J. B. Christensen, L. H. Nielsen, J. van Hest and A. Boisen, *Small*, 2024, **20**, 2403640.
20 X.-R. You, X.-J. Ju, F. He, Y. Wang, Z. Liu, W. Wang, R. Xie and L.-Y. Chu, *ACS Appl. Mater. Interfaces*, 2017, **9**, 19258–19268.
21 M. de Souza Melchiors, T. Ivanov, I. Harley, C. Sayer, P. H. H. Araújo, L. Caire da Silva, C. T. J. Ferguson and K. Landfester, *Angew. Chem., Int. Ed.*, 2022, **61**, e202207998.
22 Y. Yao, Y. Yu, X. Wan, D. Yan, Y. Chen, J. Luo, G. J. Vancso and S. Zhang, *Chem. Mater.*, 2021, **33**, 7357–7366.
23 X. Wang, J. Hu, G. Liu, J. Tian, H. Wang, M. Gong and S. Liu, *J. Am. Chem. Soc.*, 2015, **137**, 15262–15275.
24 N. P. Kamat, G. P. Robbins, J. Rawson, M. J. Therien, I. J. Dmochowski and D. A. Hammer, *Adv. Funct. Mater.*, 2010, **20**, 2588–2596.
25 H. Oliveira, E. Pérez-Andrés, J. Thevenot, O. Sandre, E. Berra and S. Lecommandoux, *J. Control. Release*, 2013, **169**, 165–170.
26 P. Wei, M. Sun, B. Yang, J. Xiao and J. Du, *J. Control. Release*, 2020, **322**, 81–94.
27 A. Napoli, M. Valentini, N. Tirelli, M. Müller and J. A. Hubbell, *Nat. Mater.*, 2004, **3**, 183–189.
28 J. Zhang, J. Hu, W. Sang, J. Wang and Q. Yan, *ACS Macro Lett.*, 2016, **5**, 919–924.
29 R. Cheng, G. Li, L. Fan, J. Jiang and Y. Zhao, *Chem. Commun.*, 2020, **56**, 12246–12249.
30 Z. Sun, G. Liu, J. Hu and S. Liu, *Biomacromolecules*, 2018, **19**, 2071–2081.
31 H. Sun, F. Meng, R. Cheng, C. Deng and Z. Zhong, *Acta Biomater.*, 2014, **10**, 2159–2168.
32 S. G. Surapaneni, S. N. Choudhari, S. V. Avhad and A. V. Ambade, *Biomater. Adv.*, 2023, **151**, 213454.
33 S. Lin, J. Shang, X. Zhang and P. Theato, *Macromol. Rapid Commun.*, 2018, **39**, 1700313.
34 S.-H. Kim, J. W. Kim, D.-H. Kim, S.-H. Han and D. A. Weitz, *Small*, 2013, **9**, 124–131.
35 F. Oroojalian, M. Babaei, S. M. Taghdisi, K. Abnous, M. Ramezani and M. Alibolandi, *J. Control. Release*, 2018, **288**, 45–61.
36 J. Du, Y. Chen, Y. Zhang, C. C. Han, K. Fischer and M. Schmidt, *J. Am. Chem. Soc.*, 2003, **125**, 14710–14711.
37 B. M. Discher, H. Bermudez, D. A. Hammer, D. E. Discher, Y.-Y. Won and F. S. Bates, *J. Phys. Chem. B*, 2002, **106**, 2848–2854.
38 Y. Li, B. S. Lokitz and C. L. McCormick, *Angew. Chem., Int. Ed.*, 2006, **45**, 5792–5795.
39 X. Wang, J. Hu and S. Liu, *Acc. Chem. Res.*, 2022, **55**, 3404–3416.
40 X. Wang, G. Liu, J. Hu, G. Zhang and S. Liu, *Angew. Chem., Int. Ed.*, 2014, **53**, 3138–3142.

41 Y. Duan, Y. Wang, X. Li, G. Zhang, G. Zhang and J. Hu, *Chem. Sci.*, 2020, **11**, 186–194.
42 G. Liu, J. Tan, J. Cen, G. Zhang, J. Hu and S. Liu, *Nat. Commun.*, 2022, **13**, 585.
43 E. Benito, L. Romero-Azogil, E. Galbis, M. V. de-Paz and M. G. García-Martín, *Eur. Polym. J.*, 2020, **137**, 109952.
44 C. Nehate, A. Nayal and V. Koul, *ACS Biomater. Sci. Eng.*, 2019, **5**, 70–80.
45 R. Nahire, M. K. Haldar, S. Paul, A. H. Ambre, V. Meghnani, B. Layek, K. S. Katti, K. N. Gange, J. Singh, K. Sarkar and S. Mallik, *Biomaterials*, 2014, **35**, 6482–6497.
46 T. Thambi, V. G. Deepagan, H. Ko, Y. D. Suh, G.-R. Yi, J. Y. Lee, D. S. Lee and J. H. Park, *Polym. Chem.*, 2014, **5**, 4627–4634.
47 Q. Song, J. Yang, S. C. L. Hall, P. Gurnani and S. Perrier, *ACS Macro Lett.*, 2019, **8**, 1347–1352.
48 J. Shen, Q. Wang, J. Fang, W. Shen, D. Wu, G. Tang and J. Yang, *RSC Adv.*, 2019, **9**, 37232–37240.
49 F. Meng, Z. Zhong and J. Feijen, *Biomacromolecules*, 2009, **10**, 197–209.
50 K. Kita-Tokarczyk, J. Grumelard, T. Haefele and W. Meier, *Polymer*, 2005, **46**, 3540–3563.
51 Y. Tu, F. Peng, P. B. White and D. A. Wilson, *Angew. Chem., Int. Ed.*, 2017, **56**, 7620–7624.
52 D. L. Rabenstein, *J. Am. Chem. Soc.*, 1973, **95**, 2797–2803.
53 M. Ishikawa, T. Ohzono, T. Yamaguchi and Y. Norikane, *Sci. Rep.*, 2017, **7**, 6909.
54 Y. Suzuki, K. H. Nagai, A. Zinchenko and T. Hamada, *Langmuir*, 2017, **33**, 2671–2676.
55 E. Brodszkij, I. N. Westensee, S. F. Holleufer, C. Ade, P. D. D. Andres, J. S. Pedersen and B. Städler, *Appl. Mater. Today*, 2022, **29**, 101549.
56 L. Jia, D. Cui, J. Bignon, A. Di Cicco, J. Wdzieczak-Bakala, J. Liu and M. H. Li, *Biomacromolecules*, 2014, **15**, 2206–2217.
57 S. Cerritelli, D. Velluto and J. A. Hubbell, *Biomacromolecules*, 2007, **8**, 1966–1972.
58 Y. He, L. Qin, Y. Huang and C. Ma, *Nanoscale Res. Lett.*, 2020, **15**, 13.

 